



Research article

Varying magnetic field strength as an effective approach to boost up the plasma signal in laser-induced breakdown spectroscopy

Atif Hussain^{a,b,*}, Syeda Tehreem Iqbal^c, Rana Muhammad Shahbaz^b, Mubeen Zafar^d, Arslan Ali Arshad^b, Komal Aslam^b, Maria Mukhtar^b^a Department of Physics, The University of Chenab, Gujrat, 50700, Pakistan^b Department of Physics, The University of Lahore, Gujrat Campus, Gujrat, 50700, Pakistan^c Department of Physics, The University of Lahore, Lahore, Pakistan^d Department of Computer Science and Information Technology, The University of Lahore, Gujrat Campus, Gujrat, 50700, Pakistan

ARTICLE INFO

Keywords:

LIBS
Spectroscopy
Excitation
Delay time
Magnetic field
Aluminium plasma

ABSTRACT

Externally variable magnetic field was incorporated with the combination of laser induced breakdown spectroscopy (LIBS) to enhance the emission characteristics of aluminum (Al) plasma. Significant emission enhancement of laser induced plasma (LIP) was obtained at different magnetic field strengths, for instance, enhancement factors of about 1.2, 1.3 and 1.4 times were observed at field-strength of 0.4, 0.5 and 0.6 T, respectively. The electron-impact excitation rates and recombination process were increased at higher field-strengths, which led to the higher emission signal due the stronger plasma confinement by the field. The electron number density and electron temperature were measured using the spectroscopic techniques at several delay times. At higher field strengths, both electron density and electron excitation temperature showed an increased trend as compared to the case when No-field was applied. Hence, the research has significance for enhancing the plasma signal which led to improve the LIBS sensitivity.

1. Introduction

LIBS is a methodical tool for optical emission spectroscopy (OES) having the capability to quantify the fundamental composition of any type of material like gas, aerosols, solids and liquids without the need of sample preparation [1]. This tool has proven its usefulness in different areas including, environmental science, artwork diagnostics, archeological object diagnosis, remote sensing capabilities, geological analysis etc. [2]. Undoubtedly, LIBS has significant uses in various scientific and industrial fields but this technique, as compared to other spectroscopic approaches, suffers problems like lower sensitivity. In order to overcome this problem, researchers proposed various different techniques to boost up the LIBS sensitivity including dual-pulse LIBS [3, 4, 5], oblique laser irradiance [6], purge gas usage [7], application of spatial and magnetic confinement [8, 9, 10, 11, 12].

The provision of magnetic field during the expansion of LIP is one of the cost-effective and simple approach to enhance the optical signal from LIBS [13, 14]. The LIP interaction with magnetic field can initiate various physical phenomena including, emission enhancement, restricted plasma free expansion, plasma instabilities, Joule heating effect, plasma

confinement, conversion of thermal energy of plasma into kinetic energy, which are accountable for increasing the electron number density and temperature in laser-generated plasma [15, 16, 17, 18, 19, 20, 21, 22, 23, 24, 25, 26]. The subject has significant utilizations in numerous extents like in extreme ultra-violet (EUV) lithographic sources, debris mitigation, thin film deposition, nanoparticle synthesization, surface modifications and LIBS detection-limits enhancement [27, 28, 29, 30, 31, 32]. The existence of magnetic field is proposed to effectively enhance the plasma parameters including plume signal strength, plasma lifetime, electron number density and electron temperature [33]. Various researchers used different experimental conditions to improve the optical signal strength of plasma generated via different materials using LIBS technology [34]. For instance, Chishti et al. investigated that emission intensity along with Al plasma parameters and reported significant enhancement across the magnetic field at all irradiances, time delays and pressures at both atmospheres of Ne and Ar. This enhancement was linked to Joule heating effect and the magnetic confinement [35]. Akhtar et. al. found that the electron number density, temperature and emission intensity were all improved when subjected to the applied-field (0.3 T). This improvement in electron temperature was associated with the magnetic compression

* Corresponding author.

E-mail addresses: atifbhatti54@gmail.com, atifbhatti54@gmail.com (A. Hussain).

and Joule heating effect while emission intensity and electron density enhancement were ascribed to the magnetic confinement of LIP [36]. Atiqa et al. measured the signal strength, number density and electron temperature of graphite across an applied transverse magnetic field with different gas pressures. The results exhibited an enhancement in emission signal and graphite plasma parameters at different ambient pressures with applied magnetic field [37]. Shen et al. successfully measured the emission enhancement factors up to 2 times for Al and 6–8 folds for copper samples under 0.8 T strength of external-field [38].

The aim of present research work was to enhance the emission parameters of laser-induced Al-plasma, concerning the excitation temperature, signal intensity, electron number density by applying the variable magnetic field. Electron number density was computed by measuring the stark broadening of neutral emission line of Al (I) 396.1 nm, while Boltzmann plot analysis was utilized to measure the excitation temperature. The time-evolution measurements of plasma parameters provide better understanding of enhanced effects because of the magnetic confinement. The experiment was performed by making use of a Nd:YAG laser. The magnetic field strength in the range of 0.2–0.6 T was generated by deploying two parallel magnets. The possible reasons for signal improvement due to the magnetic confinement of plasma were also addressed.

2. Experimental setup

Figure 1 represents the setup of the experiment. A Nd:YAG laser (Q-switched), with wavelength of 1.06 μm and having 10 Hz repetition rate with 8 ns pulse duration, was irradiated onto the rectangular shaped stripe of Al-sample (dimension 3 mm \times 1.5 mm) via a quartz lens with 100 nm focal length, for plasma generation. The laser fluence was set to 100 J/cm² corresponding to the focus point of laser beam on the surface of target, which was around 0.7 mm in diameter. For the current experiment, 100 mJ excitation energy of laser was utilized with time delay variation kept between 0.5 to 5 μs .

The rectangular samples were adjusted on a rotating translation stage in open air to deliver a new surface for the subsequent laser-ablation. The sample surface was cleaned with acetone to remove contamination before laser exposure. The two rectangular-shaped permanent magnets (60 mm \times 45 mm) were positioned 1.5 cm apart in such a way that they lie parallel to each other. The sample was located in between the poles at different locations to determine the variable magnetic field strengths (measured using a Gauss tesla device). The different combinations of magnetic field strengths were measured within the range of 0.2 T–0.6 T to improve the enhancement factors of LIP.

The OES of LIP was performed with the help of a spectrograph equipped with 2400 lines/mm diffraction gratings which collected the emitted spectra via a convex lens of focal length 75 mm. An ICCD (intensified charge coupled device) was connected with the spectrometer and spectral emission was recorded integrally within the wavelength ranges, 300 nm–316 nm and 375 nm to 415 nm, with a resolution of 0.05 nm. The ICCD gate width was kept fixed at 50 ns. A digital pulse generator was employed to synchronously trigger the laser pulse and detection system. The laser time delays and gaining parameters were adjusted through computer software which interfaced to the spectrometer. The obtained data is stored for analysis in a computer.

3. Results & discussions

Initially, the time-integrated laser-induced Al spectra were observed to examine the impact of variable applied field on the emission aspects of plasma. The optical spectra of the Al plasma were acquired within two different spectral wavelengths ranges, i.e. 300–316 nm and 375–415 nm, as shown in Figure 2. The beam of laser was concentrated onto the target surface with a time delay of 200 ns.

Figures 2(a) and 2(b) shows the emission spectra of Al-plasma at wavelength range of 300–316 nm and 375–415 nm, respectively. Each optical spectrum is recorded in the absence and with the application of varying strengths of an applied-field. A noteworthy number of Al spectral lines were identified in each spectrum as shown in Figure 2. In zero-field experiment, the spectral lines were weak but the intensity of these lines were increased significantly under the variable-field. These figures clearly demonstrated that optical signal of Al atomic lines significantly enhanced across the field-strengths. As compared to the zero-field case, the spectral lines were enhanced up to the factors of 1.2, 1.3 and 1.4 times in magnitude under field-strengths of 0.4 T, 0.5 T and 0.6 T, respectively. The major reason behind this enhancement is an upsurge in radiation recombination due to applied field strengths. Also a stronger emission signal is achieved as the volume of emitted plume species raises because of the confinement effect of applied field [39].

To understand the emission dynamics of LIP, the temporal evolution of Al atomic lines (308.25 nm and 394.33 nm) were recorded by optimizing the laser delays in the range from 100 to 5000 ns. Figures 3(a) and 3(b) reveals the line intensity of two neutral-lines as a function of delays with zero applied field and under the application of varying field-strengths (0.2–0.6 T). At a delay time of 100 ns, both atomic lines appear and their intensity starts decreasing initially, then follows an increasing trend with an increase in delay. Their emission intensity achieves maximum value at 500 ns and then reduces with any

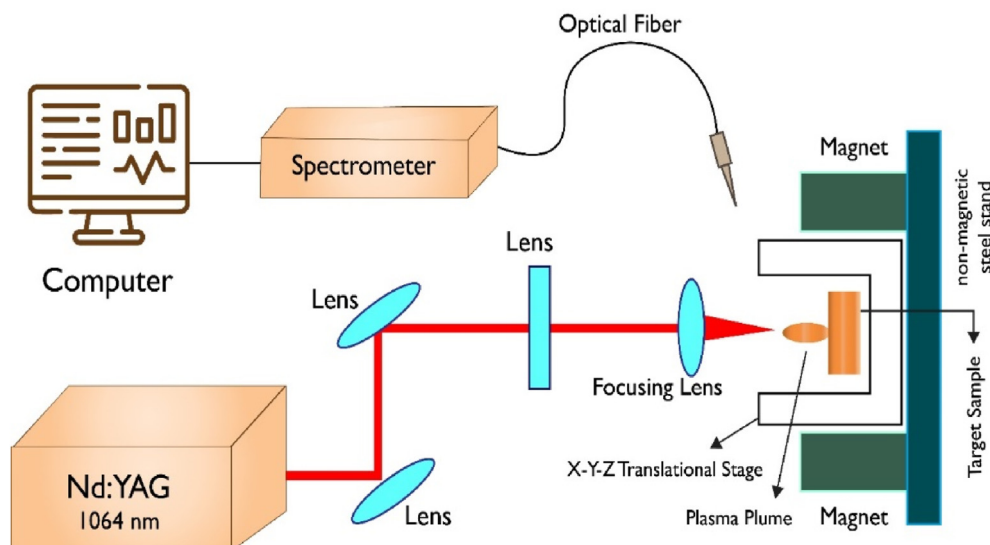


Figure 1. Experimental setup.

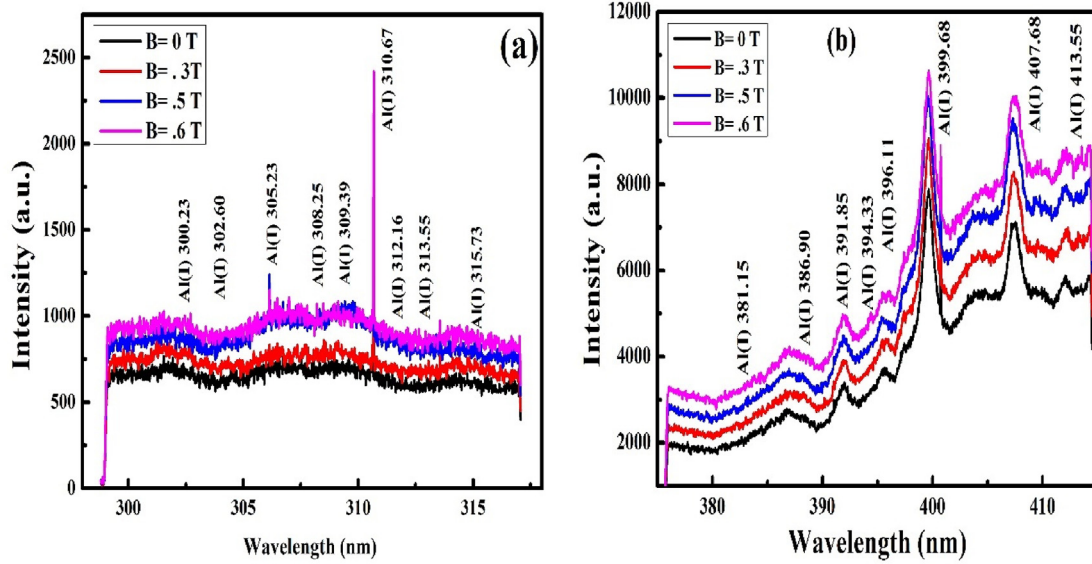


Figure 2. Emission spectrum of Al-plasma in the existence and absence of variable field (0.3, 0.5, 0.6 T) in the wavelength region from (a) 297–317 nm and (b) 377–414 nm.

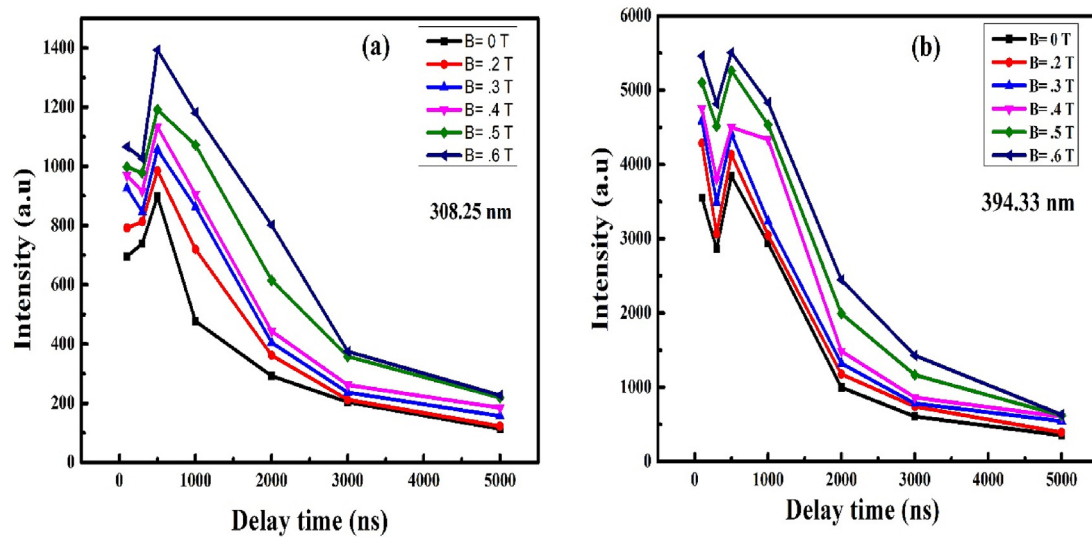


Figure 3. Temporal evolution of Al-plasma without and with the application of variable magnetic field (0.1–0.6 T) (a) 308.25 nm (b) 394.33 nm.

additional increment in delay time. With the passage of time, the plasma cooling effect occurs due to enlarged plume volume resulting in the reduction of electron temperature and plasma density, consequently, the spectral intensity decreases [40]. The lifetime of both atomic lines remains unchanged with the existence and the absence of external magnetic field due to the unchanged behavior of atomic number density. For both spectral lines, emission intensity was recorded to be higher with field-strengths at all instances. For the neutral line Al(I) 308.25 nm, the emission enhancement factors of about 1.5, 1.8, 1.9, 2.2, 2.5 in magnitude were obtained under the fields-strengths of 0.2, 0.3, 0.4, 0.5, 0.6 T, respectively. For the atomic line Al(I) 394.33 nm, the emission enhancement factors of about 1.0, 1.1, 1.4, 1.5, 1.6 were observed across the field-strengths of 0.2, 0.3, 0.4, 0.5, 0.6 T, respectively. The results declared that emission intensity of Al neutral lines was amplified because of plasma confinement by the applied field. As the plasma becomes confined across the field different processes like collision excitations, recombination rates, electron ionization and electron generation increase, which consequently enhances the plasma

intensity [41]. Moreover, when the plasma expands across the magnetic field, the ions and electrons present within plasma are detached by Lorentz force perpendicular to the applied field lines and expanding plasma [42]. As a result of separation of plasma species, a current is generated inside plume leading to a spreading out of plasma in both radian and axial directions [43]. The plume front slows down as a consequence of plasma expansion on both sides. Eq. (1) gives the expansion deceleration of plasma under the application of magnetic field [44].

$$\frac{v_2}{v_1} = \left(1 - \frac{1}{\beta}\right)^{0.5} \tag{1}$$

v_1 indicates the asymptotic velocity of expanding plasma with the provision of magnetic field and v_2 represents the velocity in absence of field. The parameter β is the analytical parameter revealing the magnetic confinement effects. The β from magneto hydrodynamic equation is written as [45],

$$\beta = \frac{8\pi n_e K_b T_e}{B^2} = \frac{\text{Plasma pressure}}{\text{Magnetic pressure}} \quad (2)$$

where the terms n_e , K_b , T_e and B shows the electron density, Boltzmann constant, electron temperature and magnetic field, respectively. According to Eq. (2) the plasma confinement occurs if the plasma and magnetic pressures becomes equal i.e., $\beta = 1$. When $\beta > 1$, the magnetic pressure is less than pressure of plasma and plasma confinement by the field would not be effective. When $\beta < 1$, the plasma can be seen in a state of magnetic confinement [38].

To further study the effectiveness of field on Al plasma, the plasma parameters were explored without and with the application of variable-field. The excitation temperature and number density of electrons are the two main factors accountable for the different ionization and excitation processes inside the plasma. These parameters are important for the plasma characterizations as they provide details concerning the physical state of plasma; the excitation of outer electrons in atom depends on the plasma temperature T_e while the electron number density N_e is crucial to assess the gas ionization degree. In this work, Boltzmann plot approach is utilized to find the excitation temperature T_e of laser-generated plasma and Stark broadening analysis is considered for the analyzation of electron density. For the calculation of T_e the plasma ought to be optically thin and should fulfill the criterion of local thermodynamic equilibrium (LTE) [44, 46]. Under LTE assumption, the excited particles obey the Boltzmann distribution. T_e is calculated by using the equation [46],

$$\ln\left(\frac{I \lambda}{gAhc}\right) = \ln\left(\frac{N(T)}{U(T)}\right) - \frac{E_m}{k T_e} \quad (3)$$

where A is used to denote the transition probability, $U(T)$ is used for partition function, K shows the Boltzmann constant, g represents the statistical weight, λ is the wavelength and I indicate the intensity. The total number density is denoted by $N(T)$ while upper level energy is represented by E_m . When the term $\ln\left(\frac{I \lambda}{gAhc}\right)$, in Eq. (3), is plotted against the values of upper lever energy, a straight-line is obtained, that is called Boltzmann constant. The slope which is equivalent to $-1/kT_e$, used to determine T_e of laser generated Al-plasma that was calculated by the specific intensities of four transition lines such as 308.16 nm, 309.25 nm, 394.21 nm and 396.01 nm [47].

N_e of the Al generated plasma was measured by choosing the stark broadening profile. In stark broadening profile, relative shapes and widths are used to compute the number density. It is measured by full-width at half-maximum (FWHM) of distinguished Stark emission line by computing the wavelength difference between two points. The N_e associated to the FWHM $\Delta\lambda_{1/2}$ of the stark broadened profile is measured by the relation [16]:

$$\Delta\lambda_{1/2} = \left[3.5A \left(\frac{N_e}{10^{16}}\right)^{1/4} [1 - N_D^{-1/3}] w + 2 \right] \left(\frac{N_e}{10^{16}}\right) w \quad (4)$$

where $\Delta\lambda_{1/2}$ is the FWHM of the Lorentzian fitted emission line, A represents the ion broadening factor, w is used to denote the electron impact width parameter while the particle number in the Debye sphere is denoted by N_D . The first term in Eq. (4) represents the ion broadening while the second term shows the electron broadening. The first term can be ignored due to its limited contribution. Consequently, Eq. (4) becomes;

$$\Delta\lambda_{1/2} = 2w \left(\frac{N_e}{10^{16}}\right) \quad (5)$$

Value of N_e can be obtained by measuring the FWHM of the transition line Al (I) 396.1 nm using Eq. (5) [48]. Figure 4 demonstrates the Lorentzian profile fit of the emission line.

The variation of T_e of Al plasma without and with the application of variable-field at various time delays (100–5000 ns) is shown in Figure 5.

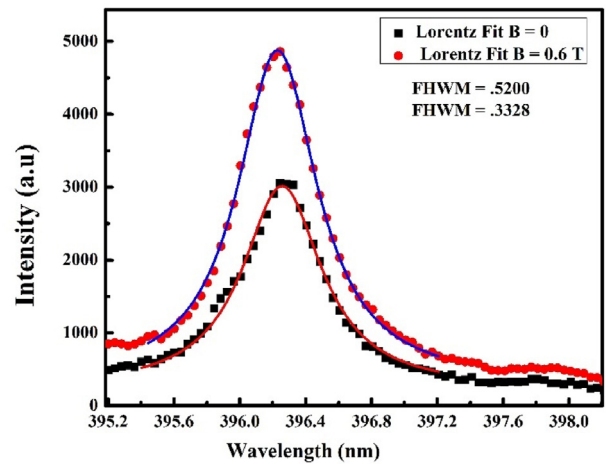


Figure 4. The Stark broadening analysis in the absence and presence of magnetic field.

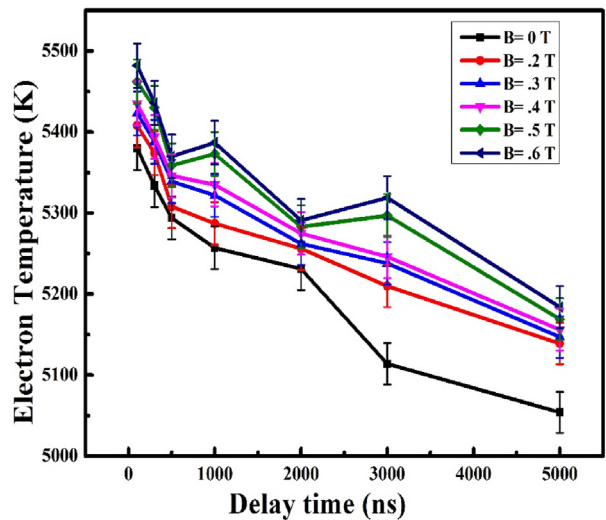


Figure 5. T_e versus varying delay times (50–1000 ns) with and without the provision of variable-field.

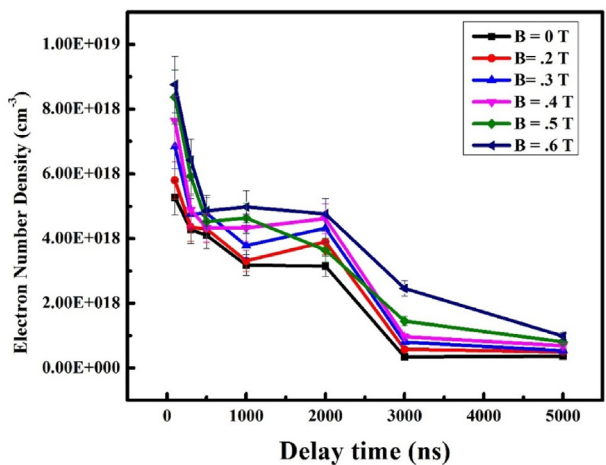


Figure 6. N_e versus the changing delay times (50–1000 ns) in the magnetic field presence and its absence.

The overall plasma temperature under both conditions was reduced with respect to the laser delays. The value of T_e in no-field case was reduced from 5380 to 5054 K, whereas T_e decreased from 5483 to 5234 K at 0.6 T field-strength. However, T_e values were greater at all applied field-strengths (0.2–0.6 T) compared to the case when no field was applied. The higher T_e across different strengths is ascribed to the adiabatic compression of plasma and joule heating effect [49]. The measured values of T_e with and without magnetic field (0.2–0.6 T) at different delays was presented in Table 1.

Table 1. Plasma parameter without and with variable magnetic field at different time delays.

Time Delay (ns)	$\Delta\lambda_{1/2}$ (FWHM)	W (T_e)	Electron Temperature (K)	Electron Number Density (N_e) 10^{18} (cm^{-3})
B = 0 T				
100	0.4412	5.2236	5380	5.2233
300	0.4468	5.2250	5334	4.2753
500	0.4488	5.2264	5294	4.1032
1000	0.3328	5.2269	5277	3.1836
2000	0.3287	5.2283	5231	3.1432
3000	0.0359	5.2315	5114	0.3438
5000	0.0388	5.2330	5051	0.37094
B= .2 T				
100	0.6056	5.2225	5408	5.7981
300	0.4546	5.2237	5374	4.3509
500	0.4492	5.2259	5308	4.2977
1000	0.3460	5.2266	5287	3.3099
2000	0.4021	5.2276	5256	3.8993
3000	0.0604	5.2290	5210	0.57411
5000	0.0519	5.2308	5139	0.4968
B= .3 T				
100	0.5060	5.2220	5423	6.8447
300	0.4971	5.2232	5388	4.7584
500	0.4998	5.2249	5339	4.7832
1000	0.3940	5.2255	5322	3.7787
2000	0.4513	5.2255	5262	4.3185
3000	0.0836	5.2281	5238	0.79964
5000	0.0558	5.2306	5147	0.53332
B= .4 T				
100	0.7975	5.2215	5435	7.6368
300	0.5107	5.2230	5394	4.8889
500	0.4526	5.2246	5346	4.3313
1000	0.4519	5.2250	5335	4.3240
2000	0.4827	5.2270	5275	4.6170
3000	0.1013	5.2278	5246	0.96876
5000	0.0722	5.2304	5156	0.69015
B= .5 T				
100	0.8736	5.2205	5462	8.3673
300	0.6186	5.2217	5430	5.9236
500	0.4723	5.2242	5359	4.5202
1000	0.3807	5.2237	5373	4.6325
2000	0.3809	5.2267	5283	3.6436
3000	0.1515	5.2263	5297	1.4491
5000	0.0846	5.2300	5169	0.80850
B= .6 T				
100	0.9142	5.2198	5482	8.7576
300	0.4617	5.2215	5436	6.4214
500	0.5076	5.2228	5370	4.8551
1000	0.5200	5.2233	5387	4.9782
2000	0.4976	5.2262	5291	4.7605
3000	0.2570	5.2256	5319	2.459
5000	0.1029	5.2296	5184	0.98345

The deviation in N_e for Al plasma as a function of different delay times (100–5000 ns) is exhibited in Figure 6. The decrease in N_e is due to the plasma cooling effects in both cases. The N_e in field-free scenario was changed from 5.26×10^{18} to 3.71×10^{17} (cm^{-3}), whereas it was changed from 8.75×10^{18} to 9.83×10^{17} (cm^{-3}) across field-strength of 0.6 T. The graph shows a substantial enhancement in electron number density across the different fields-strengths in contrast to the zero-field experiment. The possible reason for the N_e enhancement across the field is due to magnetic confinement of plasma. Consequently, the collisional rate between charged species is enhanced and a boost in plasma density can be observed [27]. The calculated values of N_e with and without magnetic field (0.2–0.6 T) at different time delays (ns) is shown in Table 1.

4. Conclusions

Summarizing, we observed the impact of variable magnetic field (0.2–0.6 T) on the emission aspects of Al plasma in order to improve the LIBS spectroscopic performance. A noteworthy impact of variable magnetic field, concerning the signal intensity and plasma parameters was detected by optimizing the delay time. It was observed that all the Al neutral lines were enhanced significantly as we increased the magnetic field strengths as compared to the zero-field experiment. The temporal profile of selected neutral lines showed distinct behavior with respect to the different field strengths. An apex of 2.5 times was obtained at 0.6 T field strength for the atomic line Al(I) 308.25 nm by optimizing the laser delay time. The possible reason for the stronger plume intensity across the applied-field could be the collisional excitations of charged species and recombination processes. Two parameters, T_e and N_e , of plasma in their temporal evolution were evaluated on the basis of spectroscopes approaches like, Boltzmann plot method and stark boarding analysis. The values of both parameters (T_e & N_e) were substantially enhanced under the impact of variable magnetic field. The effectiveness of externally applied-field was accredited to the plasma's magnetic confinement. The proposed method of plasma confinement due to the applied magnetic field, helps to enhance the detection sensitivity of LIBS.

Declarations

Author contribution statement

Atif Hussain: Conceived and designed the experiments; Performed the experiments; Analyzed and interpreted the data; Contributed reagents, materials, analysis tools or data; Wrote the paper.

Syeda Tehreem Iqbal, R M Shahbaz, Mubeen Zafar: Analyzed and interpreted the data; Wrote the paper.

Arslan Ali Arshad, Komal Aslam, Maria Mukhtar: Contributed reagents, materials, analysis tools or data.

Funding statement

This research did not receive any specific grant from funding agencies in the public, commercial, or not-for-profit sectors.

Data availability statement

Data will be made available on request.

Declaration of interest's statement

The authors declare no conflict of interest.

Additional information

No additional information is available for this paper.

References

- [1] V. Rai, S. Thakur, *Physics of Plasma in Laser-Induced Breakdown Spectroscopy, Laser-induced breakdown spectroscopy*, 2007, pp. 83–111.
- [2] W.-B. Lee, J. Wu, Y.-I. Lee, J. Sneddon, Recent applications of laser-induced breakdown spectrometry: a review of material approaches, *Appl. Spectrosc. Rev.* 39 (1) (2004) 27–97.
- [3] R. Sattmann, V. Sturm, R. Noll, Laser-induced breakdown spectroscopy of steel samples using multiple q-switch nd: yag laser pulses, *J. Phys. Appl. Phys.* 28 (10) (1995) 2181.
- [4] L. St-Onge, M. Sabsabi, P. Cielo, Analysis of solids using laser-induced plasma spectroscopy in double-pulse mode, *Spectrochim. Acta B Atom Spectrosc.* 53 (3) (1998) 407–415.
- [5] D.N. Stratis, K.L. Eland, S.M. Angel, Effect of pulse delay time on a pre-ablation dual-pulse lib plasma, *Appl. Spectrosc.* 55 (10) (2001) 1297–1303.
- [6] R.A. Multari, L.E. Foster, D.A. Cremers, M.J. Ferris, Effect of sampling geometry on elemental emissions in laser-induced breakdown spectroscopy, *Appl. Spectrosc.* 50 (12) (1996) 1483–1499.
- [7] Y. Ito, O. Ueki, S. Nakamura, Determination of colloidal iron in water by laser-induced breakdown spectroscopy, *Anal. Chim. Acta* 299 (3) (1995) 401–405.
- [8] D.A. Cremers, L.J. Radziemski, *Handbook of Laser-Induced Breakdown Spectroscopy*, John Wiley & Sons, 2013.
- [9] M. Baudelet, L. Guyon, J. Yu, J.-P. Wolf, T. Amodeo, E. Fréjafon, P. Laloi, Femtosecond time-resolved laser-induced breakdown spectroscopy for detection and identification of bacteria: a comparison to the nanosecond regime, *J. Appl. Phys.* 99 (8) (2006), 084701.
- [10] M.Z. Martin, S.D. Wullschlegler, C.T. Garten, A.V. Palumbo, Laser-induced breakdown spectroscopy for the environmental determination of total carbon and nitrogen in soils, *Appl. Opt.* 42 (12) (2003) 2072–2077.
- [11] X. Gao, J. Lin, Wavelength shift investigation of optical emission from nanosecond pulsed laser ablated metal al, *Optik* 124 (21) (2013) 4776–4779.
- [12] N. Menyuk, D.K. Killinger, C. Menyuk, Limitations of signal averaging due to temporal correlation in laser remote-sensing measurements, *Appl. Opt.* 21 (18) (1982) 3377–3383.
- [13] H. Joshi, A. Kumar, R. Singh, V. Prahlad, Effect of a transverse magnetic field on the plume emission in laser-produced plasma: an atomic analysis, *Spectrochim. Acta B Atom Spectrosc.* 65 (5) (2010) 415–419.
- [14] V.N. Rai, A.K. Rai, F.-Y. Yueh, J.P. Singh, Optical emission from laser-induced breakdown plasma of solid and liquid samples in the presence of a magnetic field, *Appl. Opt.* 42 (12) (2003) 2085–2093.
- [15] H. Pant, Laboratory simulation of space and astrophysical plasmas using intense lasers, *Phys. Scripta* 1994 (T50) (1994) 109.
- [16] S. Harilal, M. Tillack, B. O'shay, C. Bindhu, F. Najmabadi, Confinement and dynamics of laser-produced plasma expanding across a transverse magnetic field, *Phys. Rev.* 69 (2) (2004), 026413.
- [17] B. Ripin, E. McLean, C. Manka, C. Pawley, J. Stamper, T. Peyser, A. Mostovych, J. Grun, A. Hassam, J. Huba, Large-larmor-radius interchange instability, *Phys. Rev. Lett.* 59 (20) (1987) 2299.
- [18] S. Okada, K. Sato, T. Sekiguchi, Behaviour of laser-produced plasma in a uniform magnetic field—plasma instabilities, *Jpn. J. Appl. Phys.* 20 (1) (1981) 157.
- [19] L. Dirnberger, P. Dyer, S. Farrar, P. Key, Observation of magnetic-field-enhanced excitation and ionization in the plume of krf-laser-ablated magnesium, *Appl. Phys. A* 59 (3) (1994) 311–316.
- [20] D.W. Koopman, High-beta effects and anomalous diffusion in plasmas expanding into magnetic fields, *Phys. Fluid.* 19 (5) (1976) 670–674.
- [21] M. VanZeeland, W. Gekelman, S. Vincena, G. Dimonte, Production of alfvén waves by a rapidly expanding dense plasma, *Phys. Rev. Lett.* 87 (10) (2001), 105001.
- [22] S. Sudo, T. Sekiguchi, K. Sato, Re-thermalisation and flow of laser-produced plasmas in a uniform magnetic field, *J. Phys. Appl. Phys.* 11 (3) (1978) 389.
- [23] R. Tuckfield, F. Schwirzke, Dynamics of a laser created plasma expanding in a magnetic field, *Plasma Phys.* 11 (1) (1969) 11.
- [24] G. Jellison, C. Parsons, Resonant shadowgraph and schlieren studies of magnetized laser-produced plasmas, *Phys. Fluid.* 24 (10) (1981) 1787–1790.
- [25] F. Tsung, G. Morales, J. Leboeuf, Dynamics of a supersonic plume moving along a magnetized plasma, *Phys. Rev. Lett.* 90 (5) (2003), 055004.
- [26] S. Harilal, C. Bindhu, R.C. Issac, V. Nampoori, C. Vallabhan, Electron density and temperature measurements in a laser produced carbon plasma, *J. Appl. Phys.* 82 (5) (1997) 2140–2146.
- [27] W. Gekelman, M. Van Zeeland, S. Vincena, P. Pribyl, Laboratory experiments on alfvén waves caused by rapidly expanding plasmas and their relationship to space phenomena, *J. Geophys. Res.: Space Phys.* 108 (A7) (2003).
- [28] H. Kawasaki, K. Doi, S. Hiraishi, Y. Suda, Effects of cross-magnetic field on thin film preparation by pulsed nd:yag laser deposition, *Thin Solid Films* 374 (2) (2000) 278–281.
- [29] S. Harilal, B. O'Shay, M.S. Tillack, *Debris Mitigation in a Laser-Produced Tin Plume Using a Magnetic Field*, 2005.
- [30] S. Fujioka, H. Nishimura, K. Nishihara, N. Miyanaga, Y. Izawa, K. Mima, Y. Shimada, A. Sunahara, Laser production of extreme ultraviolet light source for the next generation lithography application, *Plasma Fusion Res.* 4 (2009) 48.
- [31] A. Nishihara, A. Sunahara, M. Sasaki, H. Nunami, S. Tanuma, Y. Fujioka, K. Shimada, H. Fujima, T.K. Furukawa, et al., Plasma physics and radiation hydrodynamics in developing an extreme ultraviolet light source for lithography, *Phys. Plasmas* 15 (5) (2008), 056708.
- [32] Y. Godwal, M. Taschuk, S. Lui, Y. Tsui, R. Fedosejevs, Development of laser-induced breakdown spectroscopy for microanalysis applications, *Laser Part. Beams* 26 (1) (2008) 95–104.
- [33] P. Liu, R. Hai, D. Wu, Q. Xiao, L. Sun, H. Ding, The enhanced effect of optical emission from laser induced breakdown spectroscopy of an al-li alloy in the presence of magnetic field confinement, *Plasma Sci. Technol.* 17 (8) (2015) 687.
- [34] A. Roy, S.S. Harilal, S.M. Hassan, A. Endo, T. Mocek, A. Hassanein, Collimation of laser-produced plasmas using axial magnetic field, *Laser Part. Beams* 33 (2) (2015) 175–182.
- [35] N.A. Chishti, S. Bashir, A. Dawood, M.A. Khan, Laser-induced breakdown spectroscopy of aluminum plasma in the absence and presence of magnetic field, *Appl. Opt.* 58 (4) (2019) 1110–1120.
- [36] M. Akhtar, A. Jabbar, S. Mehmood, N. Ahmed, R. Ahmed, M. Baig, Magnetic field enhanced detection of heavy metals in soil using laser induced breakdown spectroscopy, *Spectrochim. Acta B Atom Spectrosc.* 148 (2018) 143–151.
- [37] A. Arshad, S. Bashir, A. Hayat, M. Akram, A. Khalid, N. Yaseen, Q.S. Ahmad, Effect of magnetic field on laser-induced breakdown spectroscopy of graphite plasma, *Appl. Phys. B* 122 (3) (2016) 1–10.
- [38] X. Shen, Y. Lu, a.T. Gebre, H. Ling, Y. Han, Optical emission in magnetically confined laser-induced breakdown spectroscopy, *J. Appl. Phys.* 100 (5) (2006), 053303.
- [39] V.N. Rai, H. Zhang, F.Y. Yueh, J.P. Singh, A. Kumar, Effect of steady magnetic field on laser-induced breakdown spectroscopy, *Appl. Opt.* 42 (18) (2003) 3662–3669.
- [40] D.A. Cremers, L.J. Radziemski, *Laser-induced Plasmas and Applications*, Marcel Dekker, 1989.
- [41] N. Farid, S. Harilal, H. Ding, A. Hassanein, Emission features and expansion dynamics of nanosecond laser ablation plumes at different ambient pressures, *J. Appl. Phys.* 115 (3) (2014), 033107.
- [42] V. Burakov, N. Tarasenko, M. Nedelko, V. Kononov, N. Vasilev, S. Isakov, Analysis of lead and sulfur in environmental samples by double pulse laser induced breakdown spectroscopy, *Spectrochim. Acta B Atom Spectrosc.* 64 (2) (2009) 141–146.
- [43] X.K. Shen, Y. Lu, J. Sun, Spatial-confinement Effects in Laser-Induced Breakdown Spectroscopy 91, *Appl. Phys. Lett.* 2007, 081501.
- [44] H. Amamou, A. Bois, B. Ferhat, R. Redon, B. Rossetto, P. Matheron, Correction of self-absorption spectral line and ratios of transition probabilities for homogeneous and lte plasma, *J. Quant. Spectrosc. Radiat. Transf.* 75 (6) (2002) 747–763.
- [45] F.F. Chen, *Introduction to Plasma Physics*, plenum press, New York, 1974, p. 3.
- [46] C.A. Bye, A. Scheeline, Saha-Boltzmann statistics for determination of electron temperature and density in spark discharges using an echelle/ccd system, *Appl. Spectrosc.* 47 (12) (1993) 2022–2030.
- [47] A. Hussain, H. Asghar, S.T. Iqbal, M. Ishfaq, R.M. Shahbaz, Q. Riaz, Improving the spectral intensity of aluminum plasma by external magnetic field in laser-induced breakdown spectroscopy, *Optik* 251 (2022), 168220.
- [48] A. Hussain, H. Asghar, M. Tanveer, M. Zafar, Z. Nawaz, et al., Spectral emission improvement by combining ambient pressures and magnetic field-deployment in laser-induced breakdown spectroscopy, *Optik* 201 (2020), 163340.
- [49] A. Kumar, S. George, R. Singh, H. Joshi, V. Nampoori, Image analysis of expanding laser-produced lithium plasma plume in variable transverse magnetic field, *Laser Part. Beams* 29 (2) (2011) 241–247.